Applied Thermal Engineering 61 (2013) 327–333

Contents lists available at ScienceDirect

Applied Thermal Engineering

journal homepage: www.elsevier.com/locate/apthermeng

Experimental investigation on an ammonia-water based ocean thermal energy conversion system

Han Yuan, Ning Mei*, Siyuan Hu, Lu Wang, Shuai Yang

College of Engineering, Ocean University of China, 238 Songling Road, Laoshan District, Qingdao 266100, China

HIGHLIGHTS

- A test bench difference was built to study the performance of the lab-based ocean thermal energy conversion (OTEC) system.
- A horizontal tubular rising-film generator was used in the test bench.
- An orthogonal analysis was conducted to assess the impacts of operating parameter on the performance of test bench.
- The value of thermal efficiency with heating source of 30–40 °C and cooling source of 5–15 °C is 0–0.75%.

ARTICLE INFO

Article history:
Received 6 May 2013
Accepted 26 July 2013
Available online 8 August 2013

Keywords:
Ocean thermal energy conversion (OTEC)
Rising-film generator
Experimental results
Thermal efficiency

ABSTRACT

This paper used ammonia-water as the working fluid to conduct the experimental investigation on an ocean thermal energy conversion (OTEC) system. A test bench was built to study the performance of the lab-based OTEC system under different operating conditions and a horizontal tubular rising-film generator was used. Besides, an orthogonal analysis was conducted to assess the impacts of heating and cooling source temperature, as well as the solution flow rate on the performance of test bench. The results show that the heating source temperature has the most significant effects on the thermal efficiency, followed by the cooling source temperature. In contrast, the solution flow rate has little impact on the thermal efficiency. Also, higher heating source temperature leads to a relatively higher thermal efficiency. Moreover, the value of thermal efficiency with heating source of 30–40 °C and cooling source of 5–15 °C is 0–0.75%. The heat transfer temperature difference exists in generator and absorber restricts the performance improvement of the reheat power cycle.

1. Introduction

Dramatic increase of energy demand in human society has pushed us to explore new resource of energy and low-temperature heat source of such as industrial waste heat and biomass energy have been extensively utilized in power generation. Besides, another form of energy, the ocean thermal energy, has entered scientists' field of vision as a renewable and inexhaustible source of energy. The temperature difference between surface and depths of ocean is sufficient for the ocean thermal energy conversion system (OTEC) to drive a heat engine power cycle and generate power [1]. Generally, the temperature of sea water on the surface can reach to a high of 30 °C, while it can drop to a mere of 5–8 °C at 500–700 m below the surface [2]. The stability of temperature difference means that there is a potential of exploring the ocean thermal energy extensively. Meanwhile, cool water mass beneath the sea water throughout the world make it more convenient to utilize ocean thermal energy with OTEC system's help [3]. Apart from producing power, OTEC system can be used for other benefits such as producing fresh water, hydrogen, ammonia, methanol, providing air-conditioning for buildings, and even extraction of minerals [4].

In practical applications, however, there are still problems. Small temperature difference of the ocean thermal is a restriction for thermal efficiency improvement of OTEC system. Besides, the utmost efficiency of Carnot cycle is approximately 8%, which means most of the ocean thermal energy is lost. Thus, it is essential to conduct research on the improvement of the net efficiency.

Generally, the heat engine of an OTEC system can take the forms of both closed-cycle and open-cycle process. The closed-cycle commonly use a refrigerating fluid as the working fluid, which is evaporated by warm sea water and expanded through a turbine to generate power. The open-cycle operates similarly to the

* Corresponding author. Tel.: +86 532 66781105; fax: +86 532 66781550.
E-mail addresses: nmei@ouc.edu.cn, arthasmoon@163.com (N. Mei).

1359-4311/$ – see front matter © 2013 Elsevier Ltd. All rights reserved.
http://dx.doi.org/10.1016/j.applthermaleng.2013.07.050

closed-cycle except that the warm sea water acts as the working fluid. The sea water is flash-evaporated and then drives a steam turbine to produce power; meanwhile, the vapor condenses into fresh water by the cold sea water in the condenser. In the open-cycle process, the desalinated water is a byproduct of the open-cycle process [5].

Compared with the closed-cycle, the open-cycle can save exorbitant expense of building the heat exchanger. Nevertheless, requirements of such as partial vacuum operating conditions and the non-condensable prevention all increases extra power consumption [6]. All of these lead to a lower efficiency.

Basically, there are two forms of working fluid used in the closed-cycle: one is fluorocarbon; the other is binary solution of such as ammonia water. Based on this, the closed-cycle OTEC system can be divided into organic Rankine cycle and absorption power cycle. In an organic Rankine cycle, both evaporation and condensation temperature of the pure working medium remains the same. This leads to relatively higher temperature difference in evaporator and condenser, which inevitably result in a higher irreversible loss. Correspondingly, an ammonia-water based power cycle operates in a temperature variation process. It means this kind of power cycle has a relatively higher performance [7]. Research conducted by D. Wei showed that an organic Rankine cycle operates better with the heat source temperature ranges between 280 °C and 300 °C [8]. When it comes to a lower heat source temperature of 120 °C, a comparison work made by DiPippo showed that the theoretical thermal efficiency of ammonia-water cycle is higher than that of organic Rankine cycle by 3% [9].

Till now, the relatively advanced OTEC system is an ammonia-water power cycle of “Kalina cycle”, proposed by Kalina [10]. Based on this, plenty of theoretical research works were made by other scientists.

P.A. Lolos and E.D. Rogdakis [11] established a model of solar energy assisted power cycle. In this work, the thermodynamic properties of this cycle were analyzed under the conditions of operating pressure between 0.02 and 0.45 MPa and heating source temperature below 130 °C. Also, the operating parameters of gas turbine were analyzed based on the calculation results. Results showed that the thermal efficiency and the work output increase with decreasing of pressure. With solar energy’s help, the thermal efficiency was maximized to 8.3%.

“Uehara cycle”, proposed by Uehara in Saga University, is a power cycle which had got access to application. Uehara and Ikegami [12,13] conducted an optimization study of this closed-cycle OTEC system. They presented numerical results for a 100-MW OTEC plant with plate heat exchangers. The results demonstrated that the net power can reach up to 70.3% of the gross power of 100 MW for inlet warm water temperature of 26 °C and inlet coldwater temperature of 4 °C. Also, they did a performance analysis of an integrated hybrid OTEC plant [14]. The plant is a combination of a closed-cycle OTEC plant and a spray- flash desalination plant. To analyze the performance of this plant, the total heat transfer area of the heat exchangers per net power is used as an objective function. Based on this, a numerical analysis was made for a 10-MW integrated hybrid plant.

Besides, there are plenty of theoretical investigations on OTEC system [15,16]. Nevertheless, little literatures have been found on experiments of an OTEC plant. Mohammed Faizal [17] carried out an experimental study on a newly designed closed-cycle which used R134-a as the working fluid. The temperature and pressure of each state point in the test bench was measured. The result indicated that an increase in the warm water temperature increases the heat transfer between the warm water and the working fluid, thus increasing the working fluid temperature, pressure and enthalpy before the turbine. A maximum efficiency of about 1.5% was achieved in the system.

Based on above mentioned works, a reheat power cycle, which uses ammonia water as working fluid, is investigated through a series of experiments. The experimental installation presented in this paper aims at studying the performance of the lab-based OTEC system under different operating conditions. A test bench was established and an instrumentation system was used to conduct the data collection. Based on those, an orthogonal experiment was conducted to demonstrate the impact of heat source, cold source and solution flow rate on the performance of the test bench.

The originality of this work is listed as follows:

(1) A novel ammonia water based reheat power cycle was proposed in this work.
(2) A test bench working on small temperature difference was built to study the performance of the lab-based ocean thermal energy conversion (OTEC) system.
(3) A horizontal tubular rising-film generator was used in the test bench.
(4) An orthogonal analysis was conducted to assess the impacts of heating and cooling source temperature, as well as the solution flow rate on the performance of test bench.

2. Experimental step

2.1. Structure of test bench

A test bench was built to conduct the experimental study of a reheat power cycle. Fig. 1 shows a schematic of test facility. Fig. 2 shows a photograph of the experimental setup. Generally, this test bench included three main systems. One was the solution circulation system, which consists of seven major components: generator, reheater, absorber, two-stage turbines, heat exchanger, separator, as well as solution pump. Another one was water circulation system, which mainly consists of water tank and water pump. Besides, there was an instrumentation system, which mainly includes pressure gauge, flowmeter and K-type thermocouple.

The horizontal tubular rising-film generator is a device in which relatively high pressure and temperature vapor is generated by utilizing heating sources. In this test bench, two generators were installed in series. The relatively high pressure and temperature ammonia gas, along with a small amount of steam, were discharged from the generators (at state point 1), before flowing into the separator; while the weak solution in the generators was discharged (at state point 8). The ammonia gas and steam was firstly separated in the separator and then expanded through the two-stage turbines to produce power. A reheater was introduced between the two-stage turbines, which utilize warm water as the heat source. The turbine exhaust at low pressure and temperature (at state point 4) then flowed into the bubble absorber. Simultaneously, the weak solution coming from the high pressure generator was cooled in the heat exchanger and then also entered the absorber to produce the saturated solution. Chill water was utilized to exchange the thermal energy generated in the absorbing process. The heat exchanger was used to exchange heat between the weak solution and the saturated solution. The saturated solution coming from absorber (at state point 5) was pumped into the generator after heated in the heat exchanger (at state point 7) to finish the whole system.

With regard to the solution circulation system, the generator is a crucial apparatus. In this experiment, a horizontal tubular rising-film generator was chosen, and the structure chart of the generator is shown in Fig. 3. A casing reheater was used to heat the ammonia gas between the two-stage turbines. Moreover, the

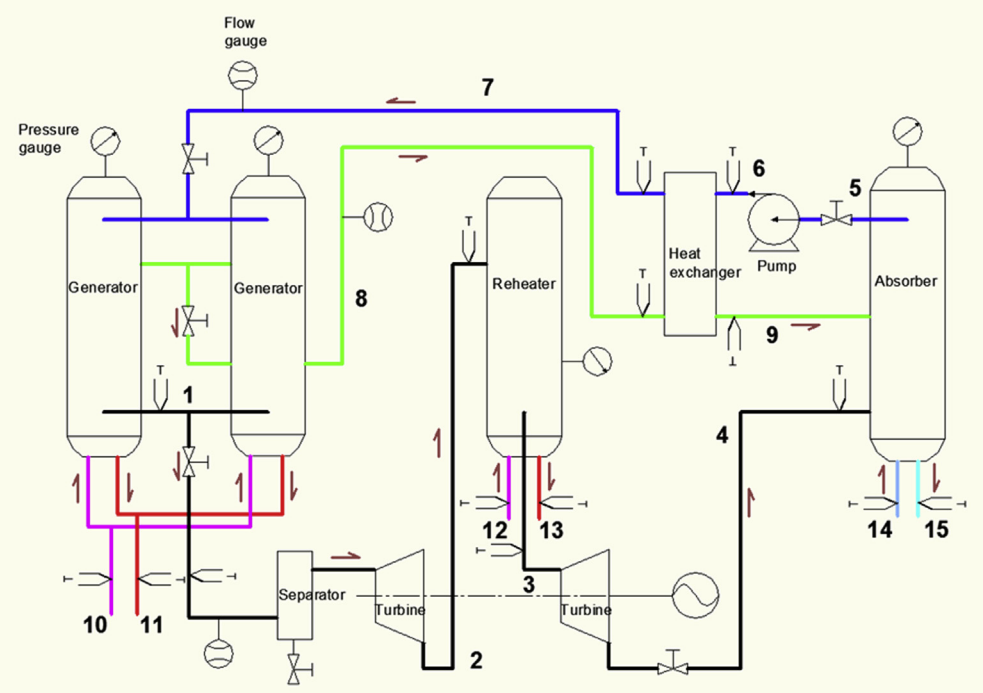

Fig. 1. Test facility schematic. Generally, this test bench concluded three main systems. One was the solution circulation system, which consists of seven major components: generator, reheater, absorber, two-stage turbines, heat exchanger, separator, as well as solution pump. The other one was water circulation system, which mainly consists of water tank and water pump. Besides, there was an instrumentation system, which mainly includes pressure gauge, flowmeter and K-type thermocouple.

bubble absorber was used to conduct the absorption process. The details of components are listed in Table 1.

2.2. Instrumentation system

A set of instruments were mounted on each component and jointed plumbing between them. These instruments consist of pressure gauge, flowmeter and K-type thermocouple. Besides, a temperature acquisition system called ADAM was used to collect data which are got by thermocouple and present them on the computer in real time. The major parameters of them are listed in Table 2.

3. Experimental plan

Orthogonal test method was used to analyze and assess the impacts of three factors on the performance of test bench. These controlled factors in this experiment were: the heating source temperature (state point 10), the cooling source temperature (state point 14) and the flow rate in solution pump (state point 7). Among them, each factor consists of three levels. Table 3 shows the experimental plan. It totaled 9 continuous tests, which lasted for 1 h respectively.

The concentration of ammonia water used in this test group was 40%. Main performance parameters of such as pressure and temperature in generator and absorber, heat flow rate during heating and cooling process, along with thermal efficiency of power cycle, were expected to gain through this experiment.

The uncertainty analysis in the measurement was conducted by using the Root–Sum–Square method [18]. The uncertainties of the turbines work and the cycle efficiencies were 2.5% and 2.8% respectively.

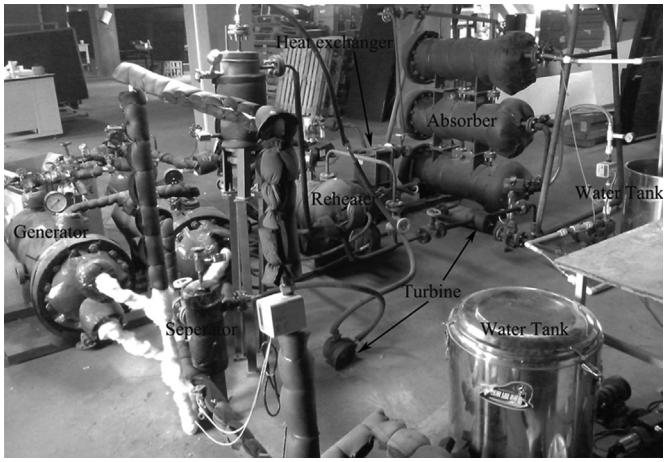

Fig. 2. A photograph of the experimental setup.

4. Experimental results and analysis

Table 4 shows the results of this experiment. The values of number listed in this table are the time–average results which were calculated based on the real time data. The output work of turbines was calculated based on the pressure, temperature and concentration of solution in both the inlets and outlets state points. Meanwhile, performance parameters of such as the heat flow rate in generator, reheater and absorber, and the thermal efficiency were all calculated based on the experiment results.

In order to reveal the effects of three factors on the thermal efficiency of power cycle, an orthogonal analysis was conducted and the result is shown in Table 5. R_A, R_B, R_C in Table 5 represents the ranges of these three factors respectively. Among these three factors of the heating source temperature, the cooling source temperature and the flow rate in solution pump, the ranking of ranges was: $R_A > R_B > R_C$, which indicates that the heating source temperature had the most significant effects on the thermal efficiency, followed by the cooling source temperature. Compared with the

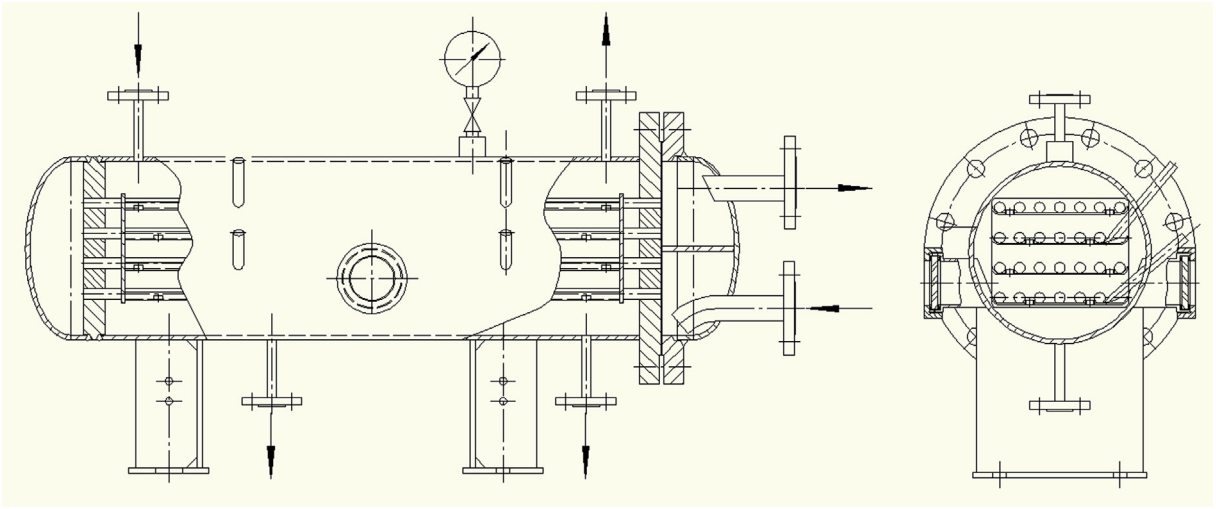

Fig. 3. Structure of horizontal tubular rising-film generator.

Table 1
Parameters of components in the experimental system.

Components	Materials	Descriptions	Structural feature
Generator	Carbon steel	Size: ϕ258 × 1068	Horizontal wire mesh tube;
		Tube: ϕ16 × 800 mm;	Double generator in parallel;
		Number: 25	Pallet structure
Reheater	Carbon steel	Size: ϕ258 × 1034	Multi-tube structure
		Tube: ϕ16 × 800 mm;	
		Number: 25	
Absorber	Carbon steel	Size: ϕ258 × 1064	Bubbling absorber
		Tube: ϕ16 × 800 mm;	
		Number: 86	
Separator	Carbon steel	Size: ϕ108 × 532	Vertical separator
Heat exchanger	Stainless steel	Heat transfer area: 2 m^2	Plate heat exchanger
		Number of plates: 41	
Turbine	Stainless steel	Number of blades: 8	
Solution pump		DC4D-3FB; 10 Bar; 0–249 L/h	Diaphragm metering pump

former two factors, the flow rate in solution pump had the least impact on the thermal efficiency.

Fig. 4 shows the heat input, heat output, as well as heat losses of the test bench. The heat input consisted of heat flow rate of both generator and reheater, while the heat output was the heat flow rate in absorber. The environmental temperature of this experiment was 10 °C, and warm water of 30–40 °C was used as heating source, which heated the ammonia water to some 30 °C. This existed temperature difference leads to heat losses in the test bench. To reduce them, the heat insulation treatment was carried out. This figure indicates that heat losses of this test bench were controlled at low-level.

Fig. 5 shows thermal efficiency of the test bench under different heating source temperature conditions. Among the test group, the heat source temperature in test 1–3 was fixed in 40 °C, compared with test 4–6 of 35 °C and test 7–9 of 30 °C. It is found that higher heating source temperature leads to a relatively higher thermal efficiency. The value of thermal efficiency with heating source of 40 °C was 0.3%–0.75%, followed by 35 °C of 0.08–0.35% and 30 °C of 0.27–0%. Meanwhile, the lateral comparison within tests of the same heating source indicated that the cooling source temperature also had a magnificent impact on the thermal efficiency of this power cycle. Lower temperature of cooling source benefited the performance of this power cycle. The similar results were got in the experimental research conducted by Mohammed Faizal [17]. Also, these results were consistent with the first law of thermodynamics.

Fig. 6 shows the volume flow rate of both rich and solution, as well as the heat flow rate of generator in each test. It was found that the lower heat flow rate in generator is associated with lower cooling source temperature. Whereas, there was no connection between the generator heat flow rate and solution volume flow rate. This phenomenon corresponded well to the orthogonal analysis results. In general, it was caused by the oversupply of rich solution which was pumped into the generator. So the value of solution flow rate had little effects on the performance of generator.

Table 2
Parameters of instruments.

K-type thermocouple	−40 to 1200 °C, ±0.1 °C
Pressure meter	0–1.5 MPa, ±0.5%
Flowmeter	0.10–10 m^3/h, ±1.5%

5. Theoretical analysis and discussion

5.1. Mathematical model

A thermodynamically model of the power cycle was developed by dividing this cycle into six simple components of such as the generator, absorber, reheater, turbine, solution pump as well as heat exchanger. Thus, the mathematical model for this power cycle is constructed.

Table 3
Experimental plan.

Factors	*A*	*B*	*C*
	Heating source temp. °C	Cooling source temp. °C	Flow rate in solution pump L/s
Test 1	40	5	0.4
Test 2	40	10	0.35
Test 3	40	15	0.3
Test 4	35	5	0.35
Test 5	35	10	0.3
Test 6	35	15	0.4
Test 7	30	5	0.3
Test 8	30	10	0.4
Test 9	30	15	0.35

Table 4
Time–average results.

	State point		Test 1	Test 2	Test 3	Test 4	Test 5	Test 6	Test 7	Test 8	Test 9
Solution loop	1	P (bar)	2.1	2.2	2.2	1.7	1.7	1.8	1.5	1.5	1.5
		T (°C)	31.5	32.2	32.1	26.4	26.8	26.9	22.3	22.9	22.9
		Qm (L s^{-1})	3.897	2.747	2.702	3.133	3.375	2.536	3.112	1.623	0.219
	2	P (bar)	1.6	1.8	2.0	1.4	1.55	1.7	1.3	1.4	1.5
		T (°C)	27.3	28.8	30.0	23.4	25.3	26.1	20.3	21.8	22.7
	3	P (bar)	1.6	1.8	2.0	1.4	1.5	1.7	1.3	1.4	1.5
		T (°C)	29.0	30.4	31.7	25.1	27.0	27.9	22.0	23.5	24.2
	4	P (bar)	1.1	1.4	1.7	1.1	1.4	1.6	1.1	1.3	1.5
		T (°C)	25.2	27.4	29.8	22.7	25.9	27.2	20.0	22.6	24.1
	5	P (bar)	1.1	1.4	1.7	1.1	1.4	1.6	1.1	1.3	1.5
		T (°C)	11.9	16.7	21.7	11.8	17.0	21.4	11.3	16.3	21.5
	6	P (bar)	2.1	2.2	2.2	1.7	1.7	1.8	1.5	1.5	1.5
		T (°C)	11.9	16.7	21.7	11.8	17.0	21.4	11.3	16.3	21.5
	7	P (bar)	2.1	2.2	2.2	1.74	1.7	1.8	1.5	1.5	1.5
		T (°C)	17.2	22.3	23.2	21.5	21.5	21.5	21.5	23.0	23.0
		Qm (L s^{-1})	0.405	0.354	0.391	0.347	0.303	0.401	0.292	0.403	0.352
	8	P (bar)	2.1	2.2	2.2	1.7	1.7	1.8	1.5	1.5	1.5
		T (°C)	31.5	32.2	32.1	26.4	26.8	26.9	22.3	22.9	22.9
		Qm (L s^{-1})	0.262	0.249	0.284	0.246	0.215	0.304	0.224	0.368	0.364
	9	P (bar)	1.9	2.0	2.0	1.5	1.5	1.6	1.3	1.3	1.4
		T (°C)	23.3	24.3	30.0	12.7	20.4	26.8	9.0	15.6	21.4
Heating/cooling loop											
Generator	10	T (°C)	40.0	40.1	40.0	35.0	34.8	35.0	30.0	30.0	29.9
	11	T (°C)	37.1	37.2	37.3	32.4	32.2	32.4	27.5	27.9	27.9
		ΔT (°C)	2.9	2.9	2.7	2.6	2.6	2.6	2.5	2.1	2.0
		Qm (L s^{-1})	2.01	1.97	2.00	2.02	1.99	1.98	2.01	1.99	2.01
		P (kW)	6.80	6.67	6.30	6.13	6.04	6.01	5.86	4.88	4.69
Reheater	12	T (°C)	40.0	40.1	40.0	35.0	34.8	35.0	30.0	30.0	29.9
	13	T (°C)	39.7	39.7	39.7	34.6	34.6	34.6	29.7	29.7	29.7
		ΔT (°C)	0.3	0.4	0.3	0.4	0.2	0.4	0.3	0.3	0.2
		Qm (L s^{-1})	0.48	0.49	0.48	0.48	0.48	0.48	0.48	0.48	0.48
		P (kW)	0.17	0.23	0.17	0.22	0.11	0.22	0.17	0.17	0.11
Absorber	14	T (°C)	5.0	10.0	15.0	4.9	10.1	15.0	5.0	9.9	15.1
	15	T (°C)	6.7	11.6	16.5	6.5	11.6	16.5	6.5	11.1	16.3
		ΔT (°C)	1.7	1.6	1.5	1.6	1.5	1.5	1.5	1.2	1.2
		Qm (L s^{-1})	3.29	3.30	3.29	3.31	3.29	3.28	3.31	3.30	3.30
		P (kW)	6.53	6.16	5.76	6.18	5.76	5.74	5.79	4.62	4.62
Solution Pump		P (W)	4.50	3.15	2.17	2.31	1.01	0.89	1.30	0.90	0.00
Turbine		P (W)	52.56	32.98	21.40	22.74	12.19	5.29	16.24	4.21	0.00
Thermal efficiency		η (%) (Calculated)	0.75	0.48	0.33	0.35	0.20	0.08	0.27	0.08	0.00

The mass and energy balance equation for the generator, absorber, reheater and heat exchanger are given as follows:

$$\Delta_{\text{out}}^{\text{in}} \sum (m_i) = 0$$

$$\Delta_{\text{out}}^{\text{in}} \sum x_i \cdot m_i = 0$$

Table 5
Orthogonal analysis result.

Factors	A	B	C	Efficiency η
	Heating source temp. °C	Cooling source temp. °C	Flow rate in solution pump L/s	
Test 1	1	1	1	0.75
Test 2	1	2	2	0.48
Test 3	1	3	3	0.33
Test 4	2	1	2	0.35
Test 5	2	2	3	0.20
Test 6	2	3	1	0.08
Test 7	3	1	3	0.27
Test 8	3	2	1	0.08
Test 9	3	3	2	0
Mean value 1	0.520	0.457	0.303	
Mean value 2	0.210	0.253	0.277	
Mean value 3	0.117	0.137	0.267	
Range	$R_A = 0.403$	$R_B = 0.320$	$R_C = 0.036$	

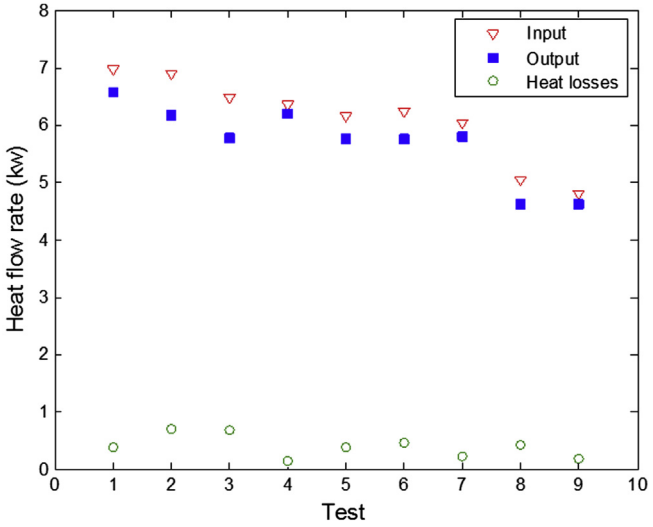

Fig. 4. Thermal balances of the test bench. The environmental temperature of this experiment was 10 °C, and warm water of 30–40 °C was used as heating source, which heated the ammonia water to some 30 °C. This existed temperature difference leads to heat losses in the test bench. To reduce them, the heat insulation treatment was carried out. This figure indicates that heat losses of this test bench were controlled at low-level.

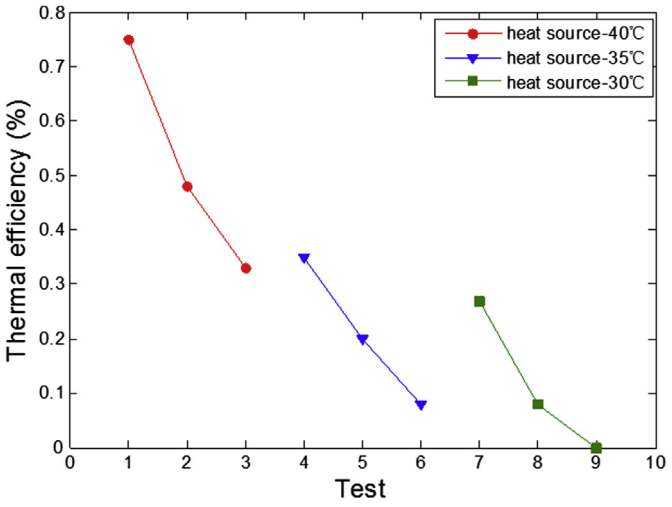

Fig. 5. Thermal efficiency of the test bench. The heat source temperature in test 1–3 was fixed in 40 °C, compared with test 4–6 of 35 °C and test 7–9 of 30 °C. It is found that higher heating source temperature leads to a relatively higher thermal efficiency. The value of thermal efficiency with heating source of 40 °C is 0.3%–0.75%, followed by 35 °C of 0.08–0.35% and 30 °C of 0.27–0%. Meanwhile, the lateral comparison within tests of the same heating source indicates that the cooling source temperature also have a magnificent impact on the thermal efficiency of this power cycle. Lower temperature of cooling source benefits the performance of this power cycle.

$$\Delta_{\text{out}}^{\text{in}}(\Sigma m_i \cdot h_i) + \Delta_{\text{out}}^{\text{in}}(\Sigma Q_j) = 0$$

where, i represents state points of 1–9; j represents components abbreviation of G, A, R.

For the turbines:

$$W_T = \eta_T m_1 (h_2 - h_1) + \eta_T m_1 (h_4 - h_3)$$

For the pump:

$$W_P = (P_G - P_A) v_A m_7 / \eta_P$$

The performance of the power cycle is evaluated by the thermal efficiency, which is defined as follows:

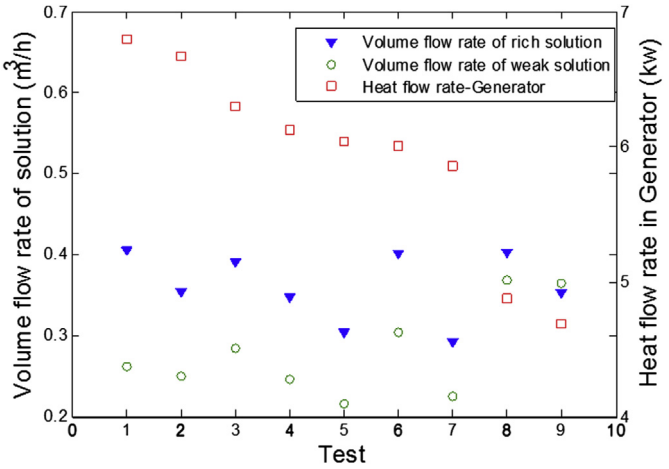

Fig. 6. Heat flow rate in generator and volume flow rate of solution. It is found that the lower heat flow rate in generator is associated with lower cooling source temperature. Whereas, there is no connection between the generator heat flow rate and solution volume flow rate. This phenomenon corresponds well to the orthogonal analysis results.

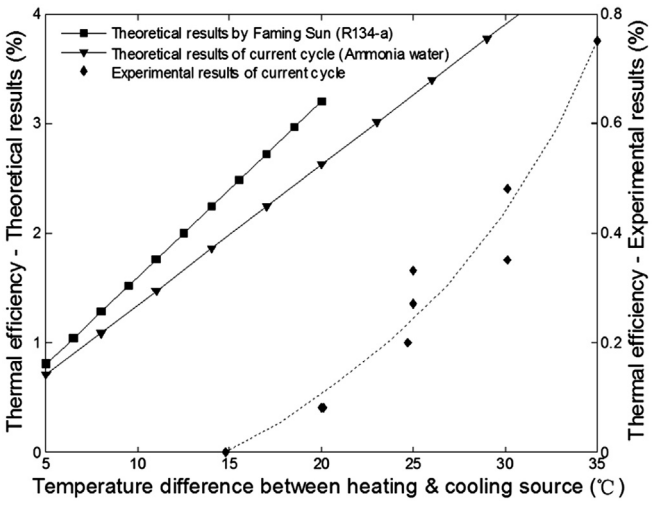

Fig. 7. Thermal efficiency under vary of temperature difference. It shows that higher temperature difference represents higher thermal efficiency. Moreover, the test bed can hardly work when the temperature difference between the heating and cooling source drop to some 15 °C.

$$\eta = \frac{W_T}{Q_G + Q_R}$$

5.2. Results comparison and discussion

Fig. 7 shows the comparison of theoretical and experimental results on temperature difference between heating and cooling source. The theoretical research conducted by Faming Sun et al. [19] was selected to compare with current work. The results showed that the theoretical thermal efficiency of both the R134-a based power cycle and current ammonia water based one saw the same trend. Higher temperature difference can lead to higher thermal efficiency. Moreover, the experimental results showed a same trend compared with the theoretical results, though the experimental thermal efficiency was much lower than the theoretical results. This was because of the heat transfer temperature difference existing in both generator and absorber. Data shown in Table 4 indicated that the generating temperature in state point (8) was much lower than heating source temperature in state point (10), with an average temperature difference of approximately 7.9 °C. It meant the test bench operates within a more narrow temperature range, which blocks the performance improvement of the power cycle. This was also the reason why the test bed could hardly work when the temperature difference between the heating and cooling source drop to some 15 °C. Therefore, it is essential to reduce the heat transfer temperature difference of both generator and absorber. Hettiarachchi [20] analyzed the relevance of operating temperatures differences to thermal efficiency and the results showed a similar trend. Also, this phenomenon was obtained by Yamada [21].

6. Conclusions

A test bench was built to study the performance of the lab-based OTEC system under different operating conditions and an orthogonal analysis was conducted to assess the impacts of heating and cooling source temperature, as well as the solution flow rate on the performance of test bench. The heating source temperature had the most significant effects on the thermal efficiency, followed by the cooling source temperature. In contrast, the solution flow rate had little

impact on the thermal efficiency. It was found that higher heating source temperature led to a relatively higher thermal efficiency. The value of thermal efficiency with heating source of 30–40 °C and cooling source of 5–15 °C was 0–0.75%. The heat transfer temperature difference existed in generator and absorber restricts the performance improvement of the reheat power cycle.

Acknowledgements

The authors acknowledge the support provided by the National Natural Science Foundation of China (NO. 51076146) and the National Key Technology Research and Development Program of the Ministry of Science and Technology of China (NO. 2012BAC25B02).

Appendix

The uncertainty analysis is based on the theory of error propagation and use Root–Sum–Square method to combine the errors and the equations are listed as follows:

$$\frac{u_\eta}{\eta} = \sqrt{\left(\frac{u_{W_T}}{W_T}\right)^2 + \left(\frac{u_{Q_G}}{Q_G}\right)^2 + \left(\frac{u_{Q_R}}{Q_R}\right)^2}$$

$$\frac{u_{W_T}}{W_T} = \sqrt{\left(\frac{u_{m_1}}{m_1}\right)^2 + \left(\frac{u_{h_1}}{h_1}\right)^2 + \left(\frac{u_{h_2}}{h_2}\right)^2 + \left(\frac{u_{h_3}}{h_3}\right)^2 + \left(\frac{u_{h_4}}{h_4}\right)^2}$$

$$\frac{u_{Q_G}}{Q_G} = \sqrt{\left(\frac{u_{m_1}}{m_1}\right)^2 + \left(\frac{u_{m_7}}{m_7}\right)^2 + \left(\frac{u_{m_8}}{m_8}\right)^2 + \left(\frac{u_{h_1}}{h_1}\right)^2 + \left(\frac{u_{h_7}}{h_7}\right)^2 + \left(\frac{u_{h_8}}{h_8}\right)^2}$$

$$\frac{u_{Q_R}}{Q_R} = \sqrt{\left(\frac{u_{m_4}}{m_4}\right)^2 + \left(\frac{u_{m_5}}{m_5}\right)^2 + \left(\frac{u_{m_9}}{m_9}\right)^2 + \left(\frac{u_{h_4}}{h_4}\right)^2 + \left(\frac{u_{h_5}}{h_5}\right)^2 + \left(\frac{u_{h_9}}{h_9}^2\right)}$$

$$u_h = \sqrt{(h(T+u_T,P)-h(T,P))^2 + (h(T,P+u_P)-h(T,P))^2}$$

References

[1] D.E. Lennard, The viability and best locations for ocean thermal energy conversion systems around the world, Renewable Energy 6 (1995) 359–365.
[2] N.J. Kim, N.C. Kim, W. Chun, Using the condenser effluent from a nuclear power plant for ocean thermal energy conversion (OTEC), Int. J. Heat Mass Transfer 36 (2009) 1008–1013.
[3] G.C. Nihous, An estimate of Atlantic Ocean thermal energy conversion (OTEC) resources, Ocean Eng. 34 (2007) 2210–2221.
[4] D. Tanner, Ocean thermal energy conversion: current overview and future outlook, Renewable Energy 6 (1995) 367–373.
[5] P.K. Takahashi, A. Trenka, Ocean thermal energy conversion: its promise as a total resource system, Energy 17 (1992) 657–668.
[6] H. Semmari, D. Stitou, S. Mauran, A novel carnot-based cycle for ocean thermal energy conversion, Energy 43 (2012) 361–375.
[7] P. Bombarda, C.M. Invernizzi, C. Pietra, Heat recovery from diesel engines: a thermodynamic comparison between Kalina and ORC cycles, Appl. Therm. Eng. 30 (2010) 212–219.
[8] D. Wei, X. Lu, Z. Lu, J. Gu, Performance analysis and optimization of organic Rankine cycle (ORC) for waste heat recovery, Energy Convers. Manage 48 (2007) 1113–1119.
[9] R. DiPippo, Second law assessment of binary plants generating power from low-temperature geothermal fluids, Geothermics 33 (2004) 565–586.
[10] A.I. Kalina, Combined cycle system with novel bottoming cycle, J. Eng. Gas Turbines Power 106 (1984) 737–742.
[11] P.A. Lolos, E.D. Rogdakis, A Kalina power cycle driven by renewable energy sources, Energy 34 (2009) 457–464.
[12] H. Uehara, Y. Ikegami, Optimization of a closed-cycle OTEC system, J. Sol. Energy Eng. 112 (1990) 247–256.
[13] N. Noda, Y. Ikegami, H. Uehara, Extraction condition of OTEC using the Uehara cycle, Int. Soc. Offshore Polar Eng. (2002) 26–31.
[14] H. Uehara, A. Miyara, Y. Ikegami, T. Nakaoka, Performance analysis of an OTEC plant and a desalination plant using an integrate hybrid cycle, J. Sol. Energy Eng. 118 (1996) 115–122.
[15] R. Deng, L. Xie, H. Lin, J. Liu, W. Han, Integration of thermal energy and seawater desalination, Energy 35 (2010) 4368–4374.
[16] P. Ahmadi, I. Dincer, M.A. Rosen, Energy and exergy analyses of hydrogen production via solar-boosted ocean thermal energy conversion and PEM electrolysis, Int. J. Hydrogen Energy 38 (2013) 1795–1805.
[17] M. Faizal, M.R. Ahmed, Experimental studies on a closed cycle demonstration OTEC plant working on small temperature difference, Renewable Energy 51 (2013) 234–240.
[18] H. Wang, R. Peterson, K. Harada, E. Miller, R. Ingram, L. Fisher, Performance of a combined organic Rankine cycle and vapor compression cycle for heat activated cooling, Energy 36 (2011) 447–458.
[19] F.M. Sun, Y. Ikegami, B.J. Jia, H. Arima, Optimization design and exergy analysis of organic rankine cycle in ocean thermal energy conversion, Appl. Ocean Res. 35 (2012) 38–46.
[20] H.D. Madhawa Hettiarachchi, M. Golubovic, W.M. Worek, Y. Ikegami, Optimum design criteria for an organic Rankine cycle using low-temperature geothermal heat sources, Energy 32 (2007) 1698–1706.
[21] N. Yamada, A. Hoshi, Y. Ikegami, Performance simulation of solar-boosted ocean thermal energy conversion plant, Renewable Energy 34 (2009) 1752–1758.